SUPPORTING INFORMATION:

Investigating E-cigarette Particle Emissions and Human Airway Depositions under Various E-cigarette Use Conditions

Yeongkwon Son[†,‡], Gediminas Mainelis[#], Cristine Delnevo[▽,&], Olivia A. Wackowski[▽,&], Stephan Schwander[†,▽,§,%], Qingyu Meng[†,▽,§*]

[†]Department of Environmental and Occupational Health, School of Public Health, Rutgers University, Piscataway, NJ, USA

[‡]Division of Atmospheric Sciences, Desert Research Institute, Reno, NV, USA

[#]Department of Environmental Sciences, Rutgers University, New Brunswick, NJ, USA

[▽]Center for Tobacco Studies, School of Public Health, Rutgers University, Piscataway, NJ, USA

[&]Cancer Prevention & Control Program, Cancer Institute of New Jersey, Rutgers University, New Brunswick NJ, USA

[§]Environmental and Occupational Health Sciences Institute, Rutgers University, Piscataway, NJ, USA

[%]Department of Urban-Global Public Health, School of Public Health, Rutgers University, Newark, New Jersey 07102

***Corresponding author:** Qingyu Meng, School of Public Health, Rutgers University, 683 Hoes Lane West, Piscataway, NJ 08854. Phone: (732) 235-9754; Fax: (732) 235-4004; Email: mengqi@sph.rutgers.edu

TABLE OF CONTENTS:

I. E-cigarette device and chemical components of flavoring ingredients (provided by the vendor/manufacturer)

Figure S1. E-cigarette device used in the study: the cartomizer (top) and battery box (bottom)

The chemical components of the flavoring ingredients were only partially released by the vendors/manufactures. The strawberry (ripe), dragon fruit, menthol, and sweet cream flavors consist of natural/artificial flavors in propylene glycol (PG). The Bavarian cream flavor consists of natural/artificial flavors, PG, and water. The cinnamon flavor is composed of artificial flavors in ethyl alcohol. The bubblegum (fruity) flavor consists of natural/artificial flavors in PG and ethyl alcohol. The graham cracker flavor is composed of natural/artificial flavor in PG and water, with caramel color, corn syrup, ethyl alcohol, and salt.

II. Vaping topography measurements

The demographics of the study participants are summarized in Table S1.

Table S1. Summary of the study participants

Number of subjects	23
Age	25 ± 10 (18-52) years
Gender	21 men and 2 women
Ethnicity	16 White; 1 Black; 3 Asian; 6 others
Duration of e-cigarette use	1.4 ± 0.9 (0.4-4.0) years

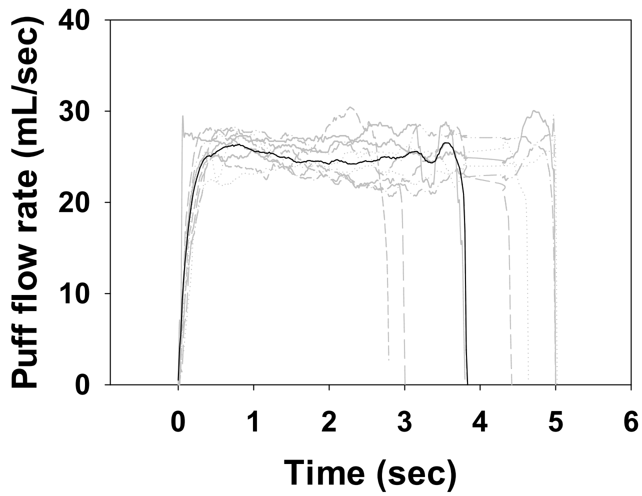

Figure S2. Observed e-cigarette puff patterns using the Cress pocket device for the study participants

III. E-cigarette particle measurement setting and data processing

The particle size distributions obtained from the PAMS and OPC were combined using weighted averages (Figure S3). In brief, particle number concentration for 0.434-1.0 μm size bin was obtained from the PAMS and 0.3-0.5 μm, 0.5-1.0 μm size bins were obtained from the OPC. Then, two size bins (0.434-0.5 μm, 0.5-1.0 μm) were reconstructed using the weighted averaging method based on the width of the size bins. In addition, particle number concentrations for the size ranges of 10-434 nm and 1.0-5.0 μm were directly obtained and used from the PAMS and OPC, respectively.

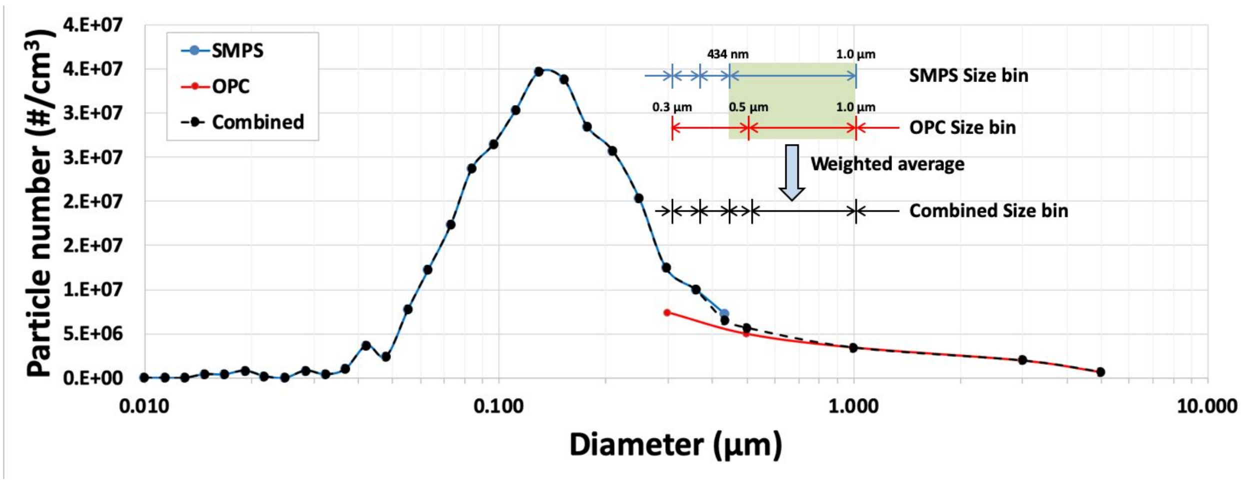

Figure S3. Merging particle size distributions obtained from the portable SMPS and the OPC

IV. Mass median diameter (MMD) calculation

The MMDs were calculated based on the measured particle count distribution and the density of e-liquids used for e-vapor generation. Briefly, density of the eight flavoring agents were measured in our lab and listed in Table S4. Then, particle mass distributions were generated based on the measured particle count distribution and the densities of e-liquids estimated using the ratio of e-liquid components (e.g. density of VG:PG=1:1 [v/v] is 1.15 g/ml). Finally, MMDs were calculated using the particle mass distribution.

Table S2. Density of VG, PG, and flavoring agents

Components	Density (g/ml)
VG	1.260
PG	1.040
Strawberry	1.030
Dragonfruit	1.040
Menthol	0.910
Cinnamon	0.950
Bubble gum	0.975
Bavarian	1.044
Sweet cream	1.072
Graham cracker	1.062

V. MPPD model assumptions and the deposition of e-cigarette particles in the human respiratory system

The input parameters for the MPPD model are specified in Table S4. In brief, the Yeh/Schum symmetric lung model was used in dosimetry modeling. The functional reserve capacity, the upper respiratory tract volume, the total inhalation volume, and the breathing periods were adopted from the ICRP (International Commission on Radiological Protection) model for human respiratory track deposition.[1] The aerosol density was set as the density of VG, PG, or the averaged density of VG and PG. Input parameters informed directly from our study include smoking topographies which are specified in Table S3, and the CMDs and GSDs of e-cigarette particles measured in our study.

Table S3. The input parameters for the MPPD model

Parameter	Value	Reference
Model type	Yeh/Schum symmetric lung	ICRP[1]
Functional reserve capacity	3,300 ml	ICRP[1]
Upper respiratory tract volume	50 ml	ICRP[1]
Total inhalation volume	500 ml	ICRP[1]
Breathing period	5 seconds	ICRP[1]
Puff volume	Obtained from this study	This study
Inhalation time	Obtained from this study	This study
Aerosol concentration	Obtained from this study	This study
Aerosol density	VG: 1.26 g/ml, PG: 1.04 g/ml, PG:VG: 1.15 g/ml	This study
Count median diameter	Obtained from this study	This study
Geometric standard deviation	Obtained from this study	This study

Since a single particle in a particle cloud is confined within the cloud and moves with the cloud, the settling velocity of the single particle equals the settling velocity of the cloud. Therefore, a cloud-equivalent particle diameter (D_c) was calculated (Equations S1-S3), so that a free particle with a diameter of D_c has the same settling velocity of a cloud, and acts like the particle cloud in terms of deposition in the upper respiratory airways.

The normalized settling velocity of a particle cloud is defined as:

$$\boldsymbol{V_c = \frac{\emptyset R^3}{F_c C_c(a)}} \qquad \textbf{Equation S1}$$

where V_c is the normalized settling velocity of a particle cloud, ϕ is the volume fraction of particles in the cloud, R is the ratio of the cloud diameter (b_0=4000 μm) and particle diameter, *a* is the half of the measured CMD, F_c is the drag force of the cloud, and C_c is the Cunningham's slip correction factor.[2]

The normalized settling velocity of a particle is defined as:

$$\boldsymbol{V_p = \frac{{D_c}^2 \rho_p g C_c}{18\mu}} \qquad \textbf{Equation S2}$$

where V_p is the settling velocity of an individual particle with the cloud-equivalent particle diameter of D_c, ρ_p is the particle density (1.26 mg/cm^3 for VG, 1.06 mg/cm^3 for PG, and 1.15 mg/cm^3 for the PG&VG mixture [PG:VG=1:1]), g is the gravity acceleration (9.8 m/s^2), and μ is the fluid viscosity.[3]

When the setting velocity of the particle cloud equals the particle with the cloud-equivalent particle diameter (i.e. $V_c = V_p$), D_c can be calculated as:

$$\boldsymbol{D_c = \sqrt{\frac{18\mu\emptyset R^3}{\rho_p g F_c C_c{}^2(a)}}} \qquad \textbf{Equation S3}$$

Finally, the measured e-cigarette particle diameter, D_p, was used to estimate the deposition of e-cigarette particles in the bronchoalveolar regions (E_{pul}); and the calculated cloud effect equivalent diameter, D_c, was employed to estimate the deposition of e-cigarette particles in the TB region (E_{TB}).

We estimated the deposition of cigarette smoke particles in the human respiratory system using the approach we proposed above, and our results was consistent with previous studies.[2, 4] Broday and Robinson[2] reported that the deposition fractions for cigarette smoke (D_p=0.25 µm, GSD=1.3, ρ=1 g/ml, N=10^9 /ml) in the TB and the bronchoalveolar regions were 0.400 and 0.220, respectively. Asgharian et al[4] reported deposition fractions of 0.600 and 0.112, respectively, in the TB and the bronchoalveolar regions for cigarette smoke (D_p=0.20 µm, GSD=1.3, ρ=1 g/ml, N=10^9 /ml). Based on the particle properties reported in Broday and Robinson[2] and Asgharian et al[4], we calculated the cloud-equivalent particle diameters using Equations S1-S3, and we estimated that the deposition fractions of cigarette particles in the TB region were 0.502 and 0.509, similar to the values reported by Broday and Robinson[2] and Asgharian et al[4], respectively.

VI. The impact of dilution on the sizes and number concentrations of e-cigarette particles

The measured CMD, GSD and particle number concentration under each dilution condition are presented in Tables S4-S8. Data presented in Tables S4-S8 were used to develop the relationship between dilution ratios and CMDs. First, the measured CMDs were regressed on pre-determined dilution ratios using polynomial regressions, and the intercept of the polynomial regression (i.e. the dilution ratio = 0) was regarded as CMD_o. Then, the association between dilution ratios and CMDs were quantified using a non-linear regression (Equation S4):

$$\frac{CMD_m}{CMD_o} = ae^{-Db} + c \qquad \textbf{Equation S4}$$

where D is the pre-determined dilution ratio; CMD_o is the estimated undiluted CMD with the polynomial regression; CMD_m is the measured CMD; and a, b, and c are the regression coefficients for the exponential decaying curve. The regression parameters are summarized in Table S9 for each particle generation condition.

Table S4. The impact of dilution on CMD (nm), GSD, and particle number concentration (NC, number of particles per cm^3) of e-cigarette particles generated under different power settings (mean ± sd; N=5)

Dilution ratio	Parameter	Device power		
		6.4W	14.7W	31.3W
548	**CMD**	202 ± 21	221 ± 15	-
	GSD	1.83 ± 0.13	1.58 ± 0.06	-
	NC	$(1.79 \pm 0.16) \times 10^8$	$(4.04 \pm 0.61) \times 10^8$	-
1068	**CMD**	164 ± 4	167 ± 15	169 ± 15
	GSD	1.89 ± 0.09	1.89 ± 0.05	1.74 ± 0.05
	NC	$(1.61 \pm 0.11) \times 10^8$	$(4.43 \pm 0.82) \times 10^8$	$(7.00 \pm 0.28) \times 10^8$
2012	**CMD**	152 ± 26	165 ± 10	158 ± 6
	GSD	2.42 ± 0.18	1.75 ± 0.04	1.76 ± 0.21
	NC	$(1.38 \pm 0.48) \times 10^8$	$(3.19 \pm 0.87) \times 10^8$	$(6.79 \pm 0.65) \times 10^8$
4179	**CMD**	143 ± 17	170 ± 11	154 ± 2
	GSD	2.70 ± 0.23	1.77±0.15	1.72 ± 0.10
	NC	$(2.35 \pm 0.89) \times 10^8$	$(2.04 \pm 0.86) \times 10^8$	$(5.20 \pm 1.06) \times 10^8$
8087	**CMD**	136 ± 13	164 ± 10	166 ± 5
	GSD	2.67 ± 0.12	1.79 ± 0.10	1.92 ± 0.09
	NC	$(2.47 \pm 0.67) \times 10^8$	$(2.54 \pm 0.71) \times 10^8$	$(6.03 \pm 0.71) \times 10^8$
15907	**CMD**	-	-	156 ± 3
	GSD	-	-	1.85 ± 0.10
	NC	-	-	$(5.70 \pm 1.12) \times 10^8$

Note: other conditions were 90 mL puff volume, 3.8 sec puff duration, 12 mg/ml nicotine in VG e-liquid

Table S5. The impact of dilution on CMD (nm), GSD, and particle number concentration (NC, number of particles per cm^3) of e-cigarette particles for 35 mL puffs (mean ± sd; N=5)

Dilution ratio	Parameter	Vaping topography (puff volume, puff duration)	
		35mL, 2sec	**35mL, 3.8sec**
396	**CMD**	159 ± 6	194 ± 9
	GSD	1.64 ± 0.20	1.50 ± 0.04
	NC	(1.94 ± 0.52) × 10^7	(7.07 ± 0.70) × 10^7
1405	**CMD**	151 ± 14	173 ± 9
	GSD	1.80 ± 0.33	1.60 ± 0.06
	NC	(1.80 ± 0.38) × 10^7	(4.66 ± 1.56) × 10^7
2097	**CMD**	128 ± 28	137 ± 13
	GSD	1.86 ± 0.90	1.55 ± 0.17
	NC	(1.82 ± 0.94) × 10^7	(3.28 ± 1.15) × 10^7
4047	**CMD**	116 ± 23	117 ± 8
	GSD	1.87 ± 0.92	1.44±0.03
	NC	(1.51 ± 0.70) × 10^7	(4.45 ± 0.99) × 10^7
8106	**CMD**	120 ± 16	120 ± 9
	GSD	1.75 ± 0.60	1.47 ± 0.04
	NC	(1.22 ± 0.35) × 10^7	(3.29 ± 0.24) × 10^7

Note: other conditions were 6.4 W power output and 12 mg/ml nicotine in VG e-liquid

Table S6. The impact of dilution on CMD (nm), GSD, and particle number concentration (NC, number of particles per cm^3) of e-cigarette particles for 90 mL puffs (mean ± sd; N=5)

Dilution ratio	Parameter	Vaping topography (puff volume, puff duration)	
		90mL, 2sec	**90mL, 3.8sec**
548	**CMD**	145 ± 5	202 ± 21
	GSD	2.50 ± 0.05	1.83 ± 0.13
	NC	(6.10 ± 0.70) × 10^7	(1.79 ± 0.16) × 10^8
1068	**CMD**	126 ± 14	164 ± 4
	GSD	2.79 ± 0.30	1.89 ± 0.09
	NC	(6.66 ± 1.32) × 10^7	(1.61 ± 0.11) × 10^8
2012	**CMD**	117 ± 7	152 ± 26
	GSD	3.60 ± 0.13	2.42 ± 0.18
	NC	(5.23 ± 0.34) × 10^7	(1.38 ± 0.48) × 10^8
4179	**CMD**	124 ± 6	143 ± 17
	GSD	3.64 ± 0.15	2.70 ± 0.23
	NC	(7.95 ± 1.16) × 10^7	(2.35 ± 0.89) × 10^8
8087	**CMD**	115 ± 8	136 ± 13
	GSD	3.78 ± 0.18	2.67 ± 0.12
	NC	(5.07 ± 0.82) × 10^7	(2.47 ± 0.67) × 10^8

Note: other conditions were 6.4 W power output and 12 mg/ml nicotine in VG e-liquid

Table S7. The impact of dilution on CMD (nm), GSD, and particle number concentration (NC, number of particles per cm^3) of e-cigarette particles for 170 mL puffs (mean ± sd; N=5)

Dilution ratio	Parameter	Vaping topography (puff volume, puff duration)	
		170mL, 2sec	170mL, 3.8sec
548	CMD	135 ± 9	-
	GSD	3.15 ± 0.22	-
	NC	(8.72 ± 0.56) × 10^7	-
1068	CMD	112 ± 10	183 ± 7
	GSD	3.16 ± 0.23	2.04 ± 0.05
	NC	(8.47 ± 0.20) × 10^7	(6.04 ± 0.37) × 10^8
2012	CMD	94 ± 8	146 ± 12
	GSD	3.21 ± 0.14	2.28 ± 0.12
	NC	(7.86 ± 0.70) × 10^7	(6.88 ± 0.45) × 10^8
4179	CMD	87 ± 12	120 ± 6
	GSD	2.82 ± 0.32	2.44 ± 0.08
	NC	(8.45 ± 1.12) × 10^7	(6.69 ± 1.15) × 10^8
8087	CMD	84 ± 6	115 ± 9
	GSD	2.61 ± 0.11	2.30 ± 0.28
	NC	(6.82 ± 3.02) × 10^7	(4.18 ± 0.45) × 10^8
15907	CMD	-	102 ± 6
	GSD	-	2.22 ± 0.22
	NC	-	(5.26 ± 0.35) × 10^8

Note: other conditions were 6.4 W power output and 12 mg/ml nicotine in VG e-liquid

Table S8. The impact of dilution on CMD (nm), GSD, and particle number concentration (NC, number of particles per cm^3) of e-cigarette particles generated from different e-liquids (mean ± sd; N=5)

Dilution ratio	Parameter	E-liquid (base material with 12 mg/mL nicotine)		
		PG	PG:VG=1:1 (v/v)	VG
548	CMD	146 ± 12	166 ± 16	202 ± 21
	GSD	2.17 ± 0.09	2.06 ± 0.12	1.83 ± 0.13
	NC	(8.72 ± 0.85) × 10^7	(2.48 ± 0.08) × 10^8	(1.79 ± 0.16) × 10^8
1068	CMD	139 ± 6	148 ± 12	164 ± 4
	GSD	2.39 ± 0.09	2.27 ± 0.10	1.89 ± 0.09
	NC	(8.62 ± 0.67) × 10^7	(1.60 ± 0.24) × 10^8	(1.61 ± 0.11) × 10^8
2012	CMD	118 ± 3	136 ± 12	152 ± 26
	GSD	2.71 ± 0.09	2.45 ± 0.13	2.42 ± 0.18
	NC	(9.25 ± 0.44) × 10^7	(2.00 ± 0.27) × 10^8	(1.38 ± 0.48) × 10^8
4179	CMD	120 ± 9	128 ± 10	143 ± 17
	GSD	2.48 ± 0.09	2.53 ± 0.09	2.70 ± 0.23
	NC	(8.34 ± 0.99) × 10^7	(2.09 ± 0.09) × 10^8	(2.35 ± 0.89) × 10^8
8087	CMD	128 ± 6	120 ± 10	136 ± 13
	GSD	2.62 ± 0.14	2.22 ± 0.11	2.67 ± 0.12
	NC	(7.75 ± 0.68) × 10^7	(2.34 ± 0.27) × 10^8	(2.47 ± 0.67) × 10^8

Note: other conditions were 6.4 W power output, 90 mL puff volume, 3.8 sec puff duration

Table S9. The regression coefficients of Equation S1 under various particle generation conditions

Category	Conditions	Parameters				R^2
		CMD_o	a	b	c	
Device setting	**6.4W***	232	0.414	-0.001	0.586	0.68
	14.7W	256	0.350	-0.001	0.650	0.57
	31.3W	259	0.384	-0.001	0.616	0.74
Topography	**35mL, 2sec**	168	0.297	0.000	0.703	0.44
	35mL, 3.8sec	211	0.440	-0.001	0.560	0.84
	90mL, 2sec	166	0.278	-0.001	0.722	0.50
	90mL, 3.8sec*	232	0.414	-0.001	0.586	0.68
	170mL,2sec	162	0.473	-0.001	0.527	0.83
	170mL, 3.8sec	223	0.511	0.000	0.489	0.30
E-liquid	**VG***	232	0.414	-0.001	0.586	0.68
	PG:VG	184	0.327	-0.001	0.673	0.64
	PG	167	0.258	-0.001	0.742	0.52

*The three conditions used identical vaping parameters to generate e-cigarette particles

VII. The impact of temperature and relative humidity on the sizes and number concentrations of e-cigarette particles

Table S10. The impact of testing temperature and relative humidity on the measured count median diameters (CMD) and number concentrations (mean ± sd) of e-cigarette particles

e-liquid	Parameter	Temperature and Relative Humidity (RH)	
		20°C and 30% RH	37°C and 95% RH
VG	**CMD (nm)**	158 ± 10	164 ± 4
	MMD (µm)	2.72 ± 0.05	3.35 ± 0.24
	Geometric Standard Deviation	1.79 ± 0.21	1.89 ± 0.09
	Number Concentration (#/cm³)	$(9.35 \pm 1.38) \times 10^7$	$(1.61 \pm 0.11) \times 10^8$
PG:VG=1:1 (v:v)	**CMD (nm)**	127 ± 16	148 ± 12
	MMD (µm)	2.68 ± 0.06	3.39 ± 0.60
	Geometric Standard Deviation	1.75 ± 0.28	2.27 ± 0.10
	Number Concentration (#/cm³)	$(7.64 \pm 0.70) \times 10^7$	$(1.60 \pm 0.24) \times 10^8$
PG	**CMD (nm)**	96 ± 7	139 ± 6
	MMD (µm)	2.62 ± 0.03	3.03 ± 0.29
	Geometric Standard Deviation	2.14 ± 0.25	2.39 ± 0.29
	Number Concentration (#/cm³)	$(3.20 \pm 0.23) \times 10^7$	$(8.62 \pm 0.67) \times 10^7$

Note: other conditions were 6.4 W power output, 90 mL puff volume, 3.8 sec puff duration, and 12 mg/ml nicotine in VG

VIII. The impact of E-liquid flavoring and nicotine on the sizes and number concentrations of e-cigarette particles

Table S11. The count median diameters, mass median diameters, and number concentrations (mean ± sd) of e-cigarette particles, generated from different flavored e-liquids

Flavor	Count Median Diameter (nm)		Mass Median Diameter (μm)		Particle Number Concentration (#/cm^3)	
	Low level	High level	Low level	High level	Low level	High level
Non-flavored	209 ± 10		3.37 ± 0.21		(1.89 ± 0.25) × 10^8	
Strawberry	183 ± 12	203 ± 24	3.18 ± 0.09	3.14 ± 0.08	(1.75 ± 0.59) × 10^8	(1.09 ± 0.42) × 10^8
Dragon fruit	185 ± 11	180 ± 18	3.20 ± 0.09	3.13 ± 0.04	(1.41 ± 0.62) × 10^8	(1.41 ± 0.42) × 10^8
Menthol	183 ± 11	187 ± 14	3.22 ± 0.08	3.20 ± 0.02	(1.09 ± 0.18) × 10^8	(9.19 ± 1.91) × 10^7
Cinnamon	186 ± 15	184 ± 13	3.20 ± 0.06	3.24 ± 0.02	(1.11 ± 0.21) × 10^8	(1.27 ± 0.05) × 10^8
Bubble gum	184 ± 16	182 ± 11	3.21 ± 0.05	3.21 ± 0.06	(1.08 ± 0.21) × 10^8	(9.82 ± 1.12) × 10^7
Bavarian	181 ± 12	188 ± 11	3.19 ± 0.07	3.20 ± 0.10	(1.31 ± 0.07) × 10^8	(1.09 ± 0.18) × 10^8
Sweet cream	187 ± 13	184 ± 8	3.19 ± 0.04	3.23 ± 0.07	(1.14 ± 0.23) × 10^8	(1.22 ± 0.17) × 10^8
Graham	186 ± 13	184 ± 11	3.23 ± 0.06	3.25 ± 0.07	(1.11 ± 0.28) × 10^8	(1.07 ± 0.21) × 10^8

Note: Low level and high level indicates 1% and 10% of flavoring agents in e-liquid, except for the cinnamon flavor (0.1% and 1% in e-liquid for low and high contents, respectively); other conditions were 6.4 W power output, 90 mL puff volume, 3.8 sec puff duration

Table S12. The count median diameters, mass median diameters, and number concentrations (mean ± sd) of e-cigarette particles, generated from e-liquids with different nicotine levels

Base material	Nicotine (mg/ml)	Count Median Diameter (nm)	Mass Median Diameter (μm)	Particle Number Concentration (#/cm^3)
VG	0	215 ± 9	3.46 ± 0.04	(2.19 ± 0.29) × 10^8
	3	215 ± 9	3.37 ± 0.22	(1.91 ± 0.19) × 10^8
	12	205 ± 5	3.35 ± 0.24	(1.61 ± 0.11) × 10^8
	24	212 ± 10	3.23 ± 0.21	(1.82 ± 0.13) × 10^8
	36	199 ± 11	3.42 ± 0.27	(1.89 ± 0.10) × 10^8
PG:VG= 1:1 (v:v)	0	173 ± 10	3.48 ± 0.21	(1.80 ± 0.16) × 10^8
	3	180 ± 7	3.44 ± 0.35	(1.71 ± 0.19) × 10^8
	12	170 ± 14	3.43 ± 0.56	(1.59 ± 0.25) × 10^8
	24	175 ± 5	3.61 ± 0.42	(1.61 ± 0.10) × 10^8
	36	179 ± 8	3.69 ± 0.35	(1.72 ± 0.16) × 10^8
PG	0	172 ± 10	3.07 ± 0.13	(1.12 ± 0.14) × 10^8
	3	159 ± 7	2.99 ± 0.09	(0.72 ± 0.06) × 10^8
	12	159 ± 7	3.03 ± 0.29	(0.86 ± 0.07) × 10^8
	24	158 ± 12	3.11 ± 0.19	(0.91 ± 0.08) × 10^8
	36	164 ± 7	3.13 ± 0.07	(0.89 ± 0.05) × 10^8

Note: other conditions were 6.4 W power output, 90 mL puff volume, 3.8 sec puff duration

IX. Estimated e-cigarette particle deposition fractions

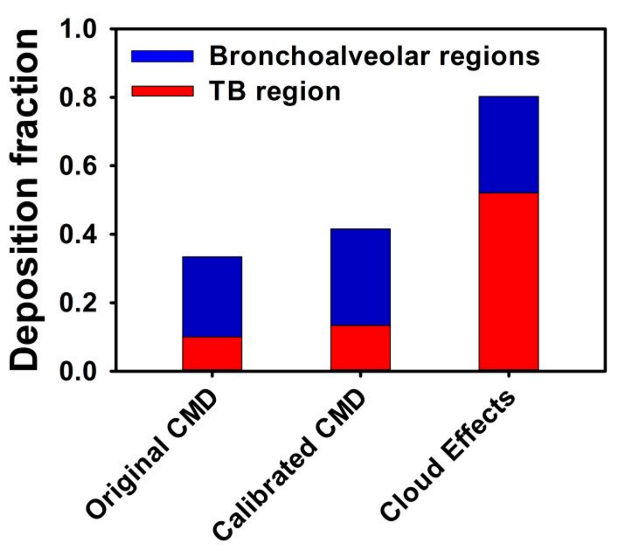

Figure S4. The deposition fractions of e-cigarette particles in the bronchoalveolar regions and the TB region, calculated with 1) the originally measured e-cigarette particle size, 2) e-cigarette particle size corrected for dilution, and 3) e-cigarette particle size corrected for both dilution and cloud effects. E-cigarette particles were generated from VG-based non-flavored e-liquids containing 12 mg/ml nicotine, under 6.4 watts, and 90 mL and 3.8 sec puffs.

Figure S5 illustrates the calculated e-cigarette particle deposition in human airways with and without cloud effects and Tables S5-S8 present modeled deposition fractions of e-cigarette particles in the TB and the bronchoalveolar regions in human airways. Similar deposition fractions in the TB and the bronchoalveolar regions were observed across different e-cigarette power outputs: 0.528 in the TB region and 0.265 in the bronchoalveolar regions, respectively, at 6.4 watts; and 0.506 in the TB region and 0.346 in the bronchoalveolar regions, respectively, at 31.3 watts. In contrast, larger puff volumes were associated with higher TB region depositions, which were 0.516, 0.528, and 0.541 for 35 ml, 90 ml, and 170 ml puffs, respectively. Deposition fractions of e-cigarette particles were similar across different e-liquids with various components.

Table S13. The deposition fraction of e-cigarette particles, generated under different e-cigarette device power in the tracheal bronchus (TB) region and the bronchoalveolar regions of human airways

Region	Power output		
	6.4W	**14.7W**	**31.3W**
TB	0.541	0.532	0.517
Bronchoalveolar	0.269	0.290	0.306

Table S14. The deposition fraction of e-cigarette particles in the tracheal bronchus (TB) region and the bronchoalveolar regions of human airways under different vaping topographies

Deposition Region	Puff Volume and Puff Duration					
	35 ml		90 ml		170 ml	
	2 sec	3.8 sec	2 sec	3.8 sec	2 sec	3.8 sec
TB	0.511	0.504	0.534	0.520	0.529	0.542
Bronchoalveolar	0.137	0.159	0.260	0.251	0.073	0.228

Table S15. The deposition fraction of e-cigarette particles, generated from e-liquid with different base material and nicotine contents, in the tracheal bronchus (TB) region and the bronchoalveolar regions of human airways

Region	Power output		
	VG	PG:VG (v:v=1:1)	PG
TB	0.530	0.538	0.539
Bronchoalveolar	0.289	0.174	0.156

Table S16. The deposition fraction of e-cigarette particles, generated from different flavored e-liquid, in the tracheal bronchus (TB) region and the bronchoalveolar regions of human airways

Flavoring Agent Content	Deposition Region	Flavoring Agents							
		Strawberry	Dragon fruit	Menthol	Cinnamon	Bubble gum	Bavarian	Sweet cream	Graham
Low	**TB**	0.523	0.526	0.534	0.531	0.526	0.532	0.534	0.533
	Broncho-alveolar	0.265	0.273	0.283	0.284	0.284	0.281	0.283	0.282
High	**TB**	0.549	0.530	0.529	0.527	0.538	0.539	0.531	0.534
	Broncho-alveolar	0.290	0.273	0.287	0.278	0.288	0.286	0.284	0.281

Note: Low level and high level flavoring agents indicate 1% and 10% of flavoring agents in e-liquids, except for the cinnamon flavor (0.1% and 1% in e-liquids for low and high contents, respectively)

References

(1) ICRP. (1994) *Human Respiratory Tract Model for Radiological Protection.* . ICRP Publication 66. Ann. ICRP 24 (1-3).

(2) Broday, D. M., and Robinson, R. (2003) Application of cloud dynamics to dosimetry of cigarette smoke particles in the lungs. *Aerosol Science & Technology 37(6)*, 510-527.

(3) Hinds, W. C. (2012) *Aerosol technology: properties, behavior, and measurement of airborne particles*. John Wiley & Sons, Hoboken, NJ, USA.

(4) Asgharian, B., Price, O. T., Yurteri, C. U., Dickens, C., and McAughey, J. (2014) Component-specific, cigarette particle deposition modeling in the human respiratory tract. *Inhalation toxicology 26(1)*, 36-47.